A new chaotic system with axe-shaped equilibrium, its circuit implementation and adaptive synchronization

SUNDARAPANDIAN VAIDYANATHAN, ACENG SAMBAS and MUSTAFA MAMAT

In the recent years, chaotic systems with uncountable equilibrium points such as chaotic systems with line equilibrium and curve equilibrium have been studied well in the literature. This reports a new 3-D chaotic system with an axe-shaped curve of equilibrium points. Dynamics of the chaotic system with the axe-shaped equilibrium has been studied by using phase plots, bifurcation diagram, Lyapunov exponents and Lyapunov dimension. Furthermore, an electronic circuit implementation of the new chaotic system with axe-shaped equilibrium has been designed to check its feasibility. As a control application, we report results for the synchronization of the new system possessing an axe-shaped curve of equilibrium points.

Key words: chaos, chaotic systems, curve equilibrium, Lyapunov exponents, circuit design, synchronization

1. Introduction

It is well-known that chaos theory has been applied to several areas such as such as lasers [1, 2], memristors [3, 4], chemical reactions [5, 6], finance [7], oscillators [8–15], neural networks [16], ecology [17], biology [18, 19], weather systems [20, 21], electrical circuits [22–27], sound encryption [28], image encryption [29], cryptosystems [30], robotics [31], secure communication devices [32, 33], etc.

An important area in chaos theory is the modelling of chaotic systems with infinite number of rest points (or equilibrium points) such as line rest points [34–36] or closed curve of rest points such as circle [37], square [38], rounded square [39], rectangle [40], cloud-shaped curve [41], etc.

Sundarapandian Vaidyanathan is with Research and Development Centre, Vel Tech University, 400 Feet Outer Ring Road, Avadi, Chennai-60002, Tamil Nadu, India. E-mail: sundarcontrol@gmail.com

A. Sambas is with Faculty of Informatics and Computing, Universiti Sultan Zainal Abidin, Malaysia, and Department of Mechanical Engineering, Universitas Muhammadiyah Tasikmalaya, Indonesia. E-mail: acengs@umtas.ac.id

M. Mamat is with Faculty of Informatics and Computing Universiti Sultan Zainal Abidin Gong Badak, 21300 Kuala Terengganu, Terengganu, Malaysia. E-mail: must@unisza.edu.my

Recent research on chaos modelling has shown that the chaotic systems with infinite number of rest points can be classified as special chaotic systems with hidden attractors [42, 43]. Hence, discovery of chaotic systems with line equilibrium or closed curve equilibrium is an important research topic. The synchronization of the chaotic systems has useful applications in the control literature [44–47].

In this work, we report a new chaotic system with a closed curve of equilibrium points, which has the shape of an axe. We present the system dynamics, phase plots, and analysis of the chaotic system with axe-shaped equilibrium. Furthermore, we provide a circuital implementation of the chaotic system with axe-shaped equilibrium. As a control application, we report results for the synchronization of the new system possessing an axe-shaped curve of equilibrium points.

2. A new chaotic system with an axe-shaped curve of equilibrium points

Recently, Pham *et al.* [39] have reported a general model of dynamical systems given by

$$\begin{cases} \dot{x} = z, \\ \dot{y} = -zf(x,y,z), \\ \dot{z} = g(x,y), \end{cases} \tag{1}$$

where $f(x,y,z)$ and $g(x,y)$ are two arbitrary nonlinear functions.

We get the rest points of the general model (1) by solving the equations:

$$z = 0, \tag{2a}$$

$$-zf(x,y,z) = 0, \tag{2b}$$

$$g(x,y) = 0. \tag{2c}$$

It is clear from (2a) that $z = 0$ for any rest point of the system (1).

Thus, we deduce from (2b) and (2c) that the rest points of the system (1) lie on the curve $g(x,y) = 0$ on the plane $z = 0$.

Hence, by a suitable choice of the functions $f(x,y,z)$ and $g(x,y)$, we can construct numerous dynamical systems with different types of open or closed curves of rest points.

In this paper, we choose the functions as

$$\begin{cases} f(x,y,z) = -x^2 - ay + by^2 + cxz, \\ g(x,y) = 4|x| + 4|y| + xy - 10, \end{cases} \tag{3}$$

which leads to the system

$$\begin{cases} \dot{x} &= z, \\ \dot{y} &= -z(-x^2 - ay + by^2 + cxz), \\ \dot{z} &= 4|x| + 4|y| + xy - 10. \end{cases} \quad (4)$$

Thus, the rest points of the new system (4) are described by the closed curve

$$z = 0, \qquad 4|x| + 4|y| + xy - 10 = 0, \quad (5)$$

which is an axe-shaped curve in the (x,y)-plane as shown in Figure 1. It is observed that the axe-shaped curve (Figure 1) is very different from the basic closed shapes like circle, square, rounded square and cloud [37–41].
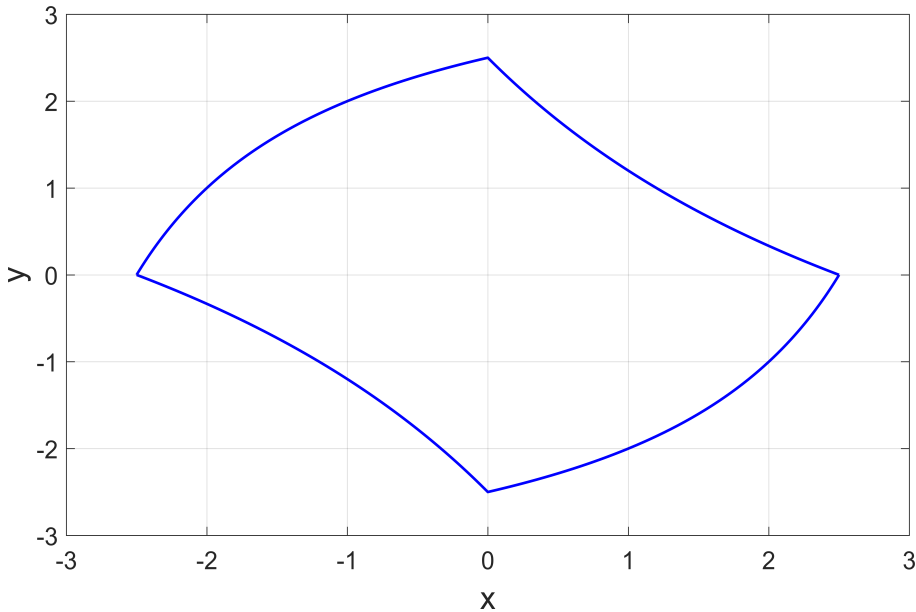

Figure 1: Axe-shaped curve of rest points of the system (4)

For the choice $(a,b,c) = (6,0.2,0.1)$, we show that the system (4) is chaotic.

For numerical simulations of phase plots and for the calculation of Lyapunov chaos exponents, we take $X(0) = (0,0,0.2)$ and $(a,b,c) = (6,0.2,0.1)$. The chaos nature of (4) is guaranteed by the Lyapunov exponents calculated using Wolf's algorithm [49] for $T = 5000s$ as

$$L_1 = 0.11867 > 0, \qquad L_2 = 0, \qquad L_3 = -0.13175 < 0. \quad (6)$$

For the system (4), $L_1 + L_2 + L_3 = -0.01308 < 0$.

Thus, the system (4) is *dissipative*.

The local finite-time Lyapunov dimension [48] of the system (4) is esti-
mated as

$$D_L = 2 + \frac{L_1 + L_2}{|L_3|} = 2.9007. \tag{7}$$

We observe high complexity of the system (4) with axe-shaped equilibrium
by the high value of the Lyapunov dimension D_L.

It is observed that the system (4) is invariant under the change of coordinates
$(x, y, z) \mapsto (-x, -y, -z)$ for all values of the parameter set (a, b, c). This shows
that the system (4) has point reflection symmetry about the origin in $\mathbf{R}^3$. Hence,
if $(x(t), y(t), z(t))$ is a trajectory of the system (4), then $(-x(t), -y(t), -z(t))$ will
be also a trajectory of the system (4).

Figures 2–5 show the phase plots of the new chaotic attractor (4) for $X(0) =$
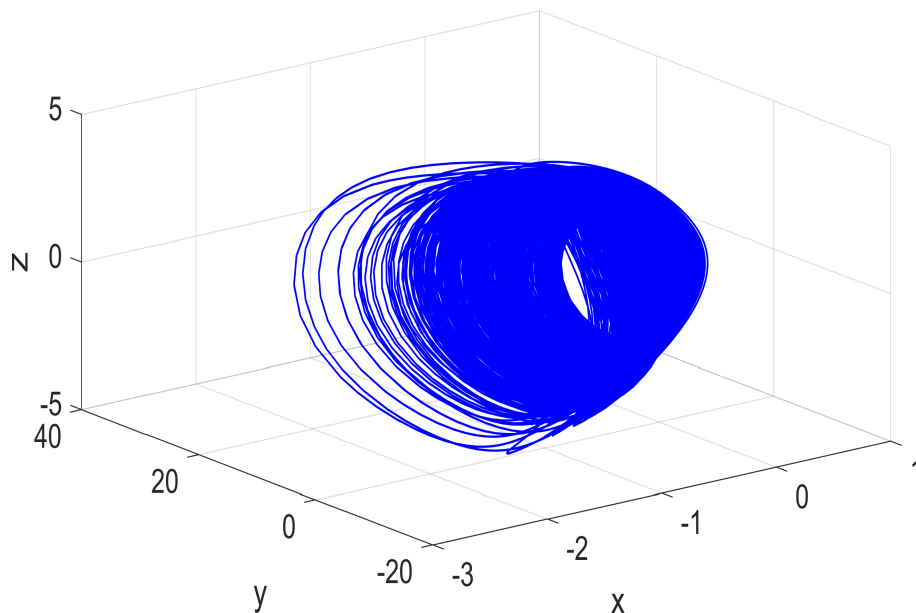$(0, 0, 0.2)$ and $(a, b, c) = (6, 0.2, 0.1)$.

Figure 2: MATLAB simulation of (4) for $X(0) = (0, 0, 0.2)$ and $(a, b, c) =$
$(6, 0.2, 0.1)$

The bifurcation diagram of the system (4) is illustrated in Figure 6. In addi-
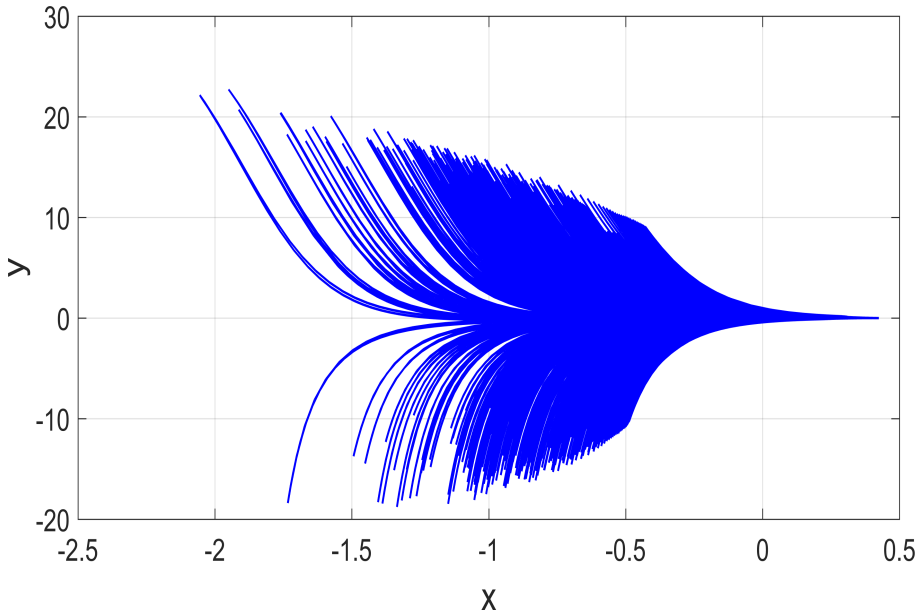tion, Poincaré map in Figure 7 also displays chaotic property of the system (4).

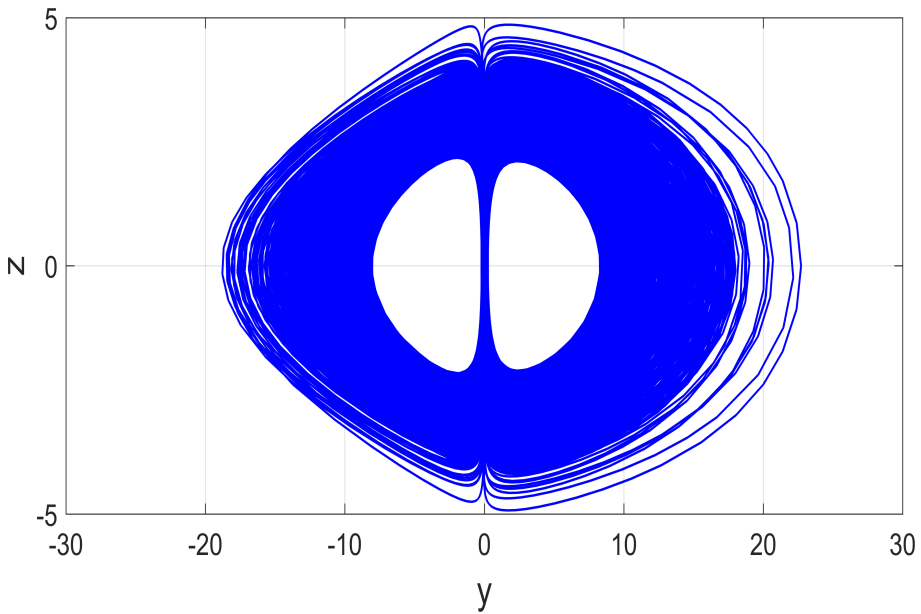Figure 3: MATLAB simulation of (4) in (x,y)-plane for $X(0) = (0,0,0.2)$ and $(a,b,c) = (6,0.2,0.1)$

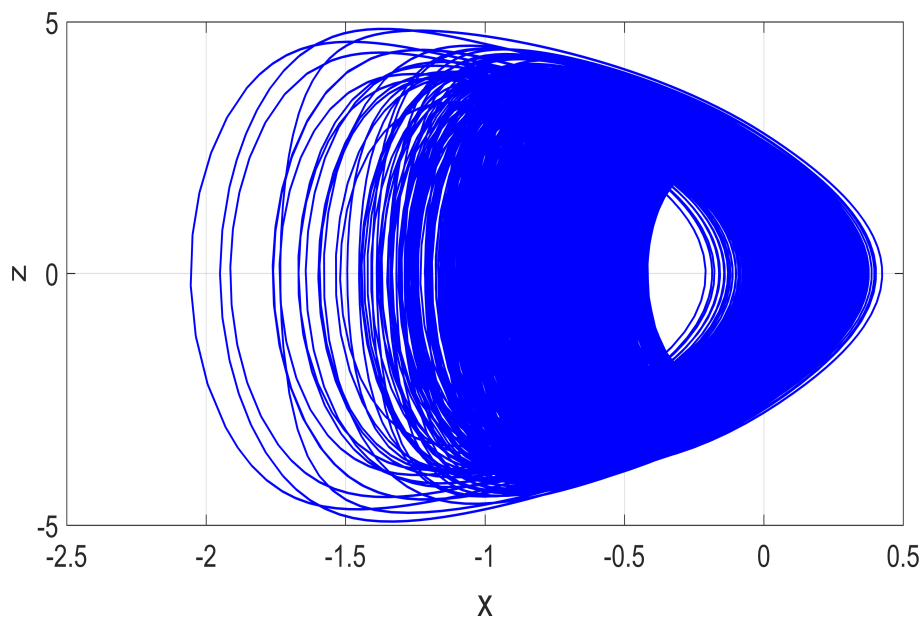Figure 4: MATLAB simulation of (4) in (y,z)-plane for $X(0) = (0,0,0.2)$ and $(a,b,c) = (6,0.2,0.1)$

Figure 5: MATLAB simulation of (4) in (x,z)-plane for $X(0) = (0,0,0.2)$ and $(a,b,c) = (6,0.2,0.1)$
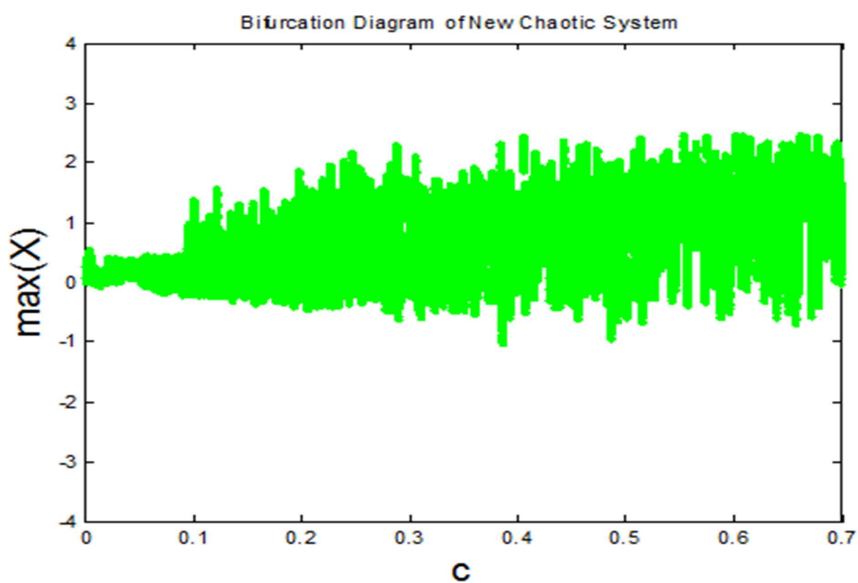

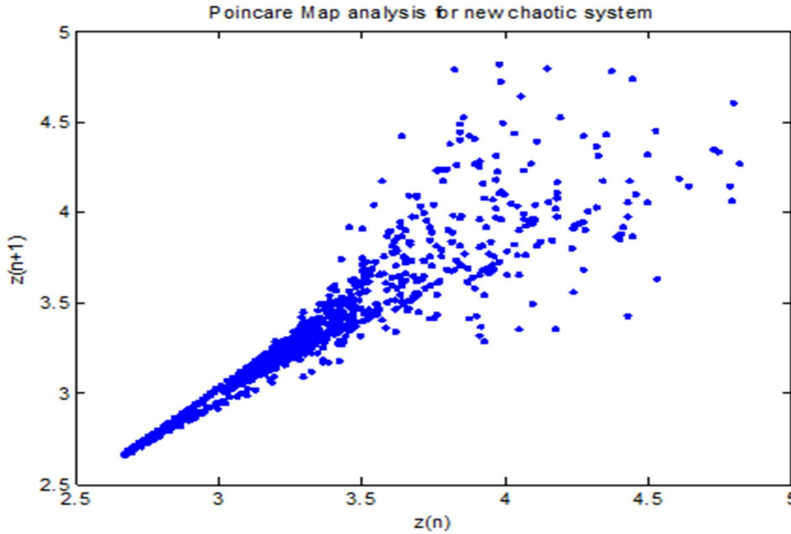Figure 6: Bifurcation diagram of (4) with respect to the bifurcation parameter c when $a = 6$ and $b = 0.2$

Figure 7: Poincaré map of (4) in the plane $z(n+1)$ versus $z(n)$ for $(a,b,c) = (6,0.2,0.1)$

3. Circuit realization of the system with axe-shaped equilibrium points

In this section, the system (4) with axe-shaped equilibrium is realized by an electronic circuit shown in Figure 8. The main circuit that realizes the system (4), has three integrators (U1A,U3A, U5A), four inverting amplifiers (U2A, U4A, U6A, U10A), one absolute function by $|x|$ signal (U8A, U9A) and one absolute function by $|y|$ signal (U7A,U11A). The state $X = (x,y,z)$ of the system (4) is characterized by the voltage across the capacitors (C_1,C_2,C_3). For the scale setting on the circuit, we can use the amplitude control method [25–27]. Thus, the system (4) is changed into the following system.
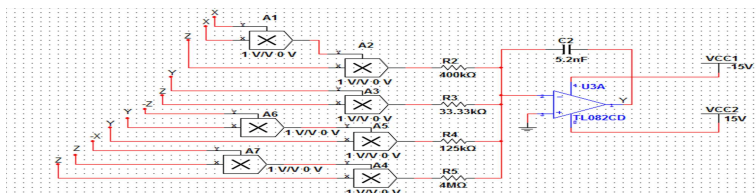
$$\begin{cases} \dot{x} &= z, \\ \dot{y} &= z(-x^2 - 2ay + 16by^2 + cxz), \\ \dot{z} &= 4|x| + 16|y| + 8xy - 5. \end{cases} \tag{8}$$

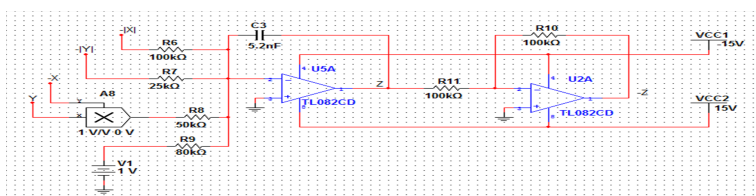Applying the Kirchhoff's laws, the circuit of Figure 8 is described by the following equations:

$$\begin{aligned} \dot{x} &= \frac{1}{C_1 R_1} z, \\ \dot{y} &= -\frac{1}{C_2 R_2} zx^2 - \frac{1}{C_2 R_3} zy + \frac{1}{C_2 R_4} zy^2 + \frac{1}{C_2 R_5} xz^2, \\ \dot{z} &= \frac{1}{C_3 R_6} |x| + \frac{1}{C_3 R_7} |y| + \frac{1}{C_3 R_8} xy - \frac{1}{C_3 R_9} V_1. \end{aligned} \tag{9}$$
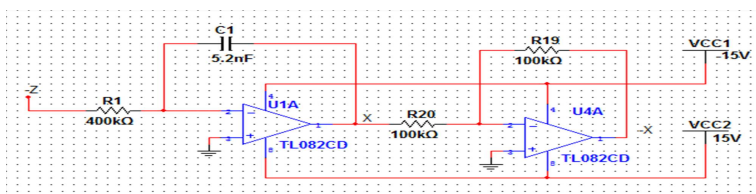
(a)

(b)

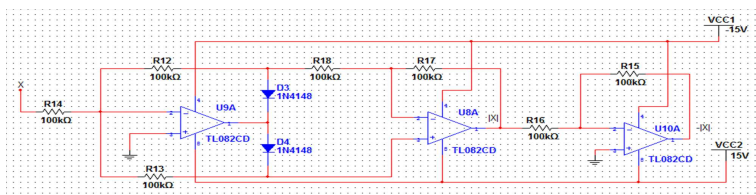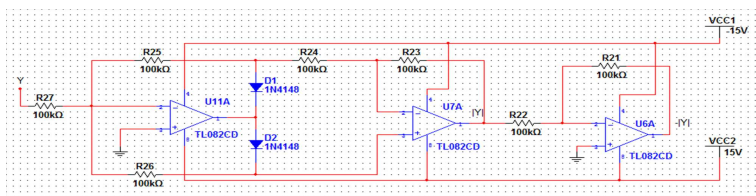

(c)

(d)

(e)

Figure 8: Circuit design of (4): (a) X signal, (b) Y signal, (c) Z signal, (d) $|X|$ signal and (e) $|Y|$ signal

The electronic components are chosen as: $R_1 = R_2 = 400$ KΩ, $R_3 = 33.33$ KΩ, $R_4 = 125$ KΩ, $R_5 = 4$ MΩ, $R_7 = 25$ KΩ, $R_8 = 50$ KΩ, $R_9 = 80$ KΩ, $R_6 = R_{10} = R_{11} = R_{12} = R_{13} = R_{14} = R_{15} = R_{16} = R_{17} = R_{18} = R_{19} = R_{20} =$

$R_{21} = R_{22} = R_{23} = R_{24} = R_{25} = R_{26} = R_{27} = 100 \text{ K}\Omega, C_1 = C_2 = C_3 = 5.2 \text{ nF}$
and $V_1 = 1V_{DC}$. Oscilloscope phase portraits of the circuit are represented in Figures 9–11. It is easy to see the good agreement between MATLAB simulation results (Figures 3–5) and the circuit simulation results (Figures 9–11).
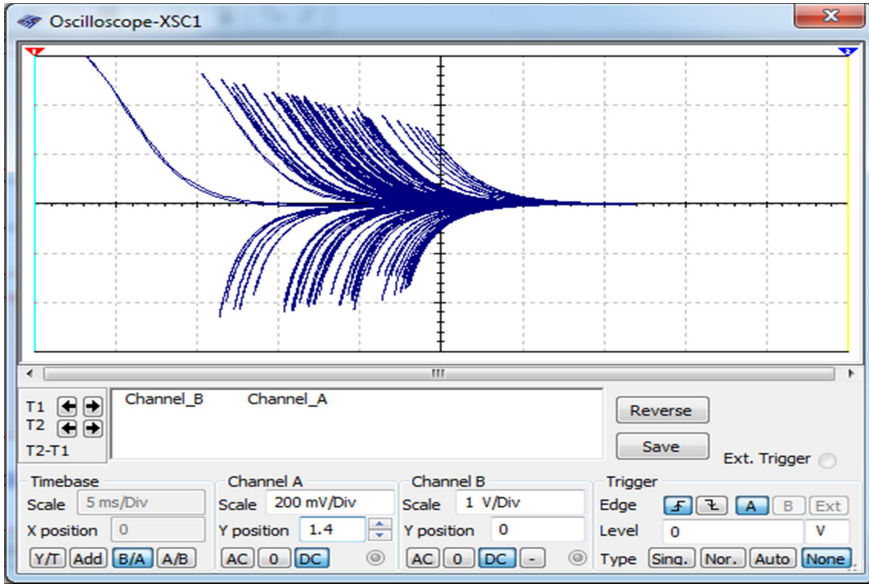

Figure 9: MultiSIM 10 simulation of the system in (x, y)-plane
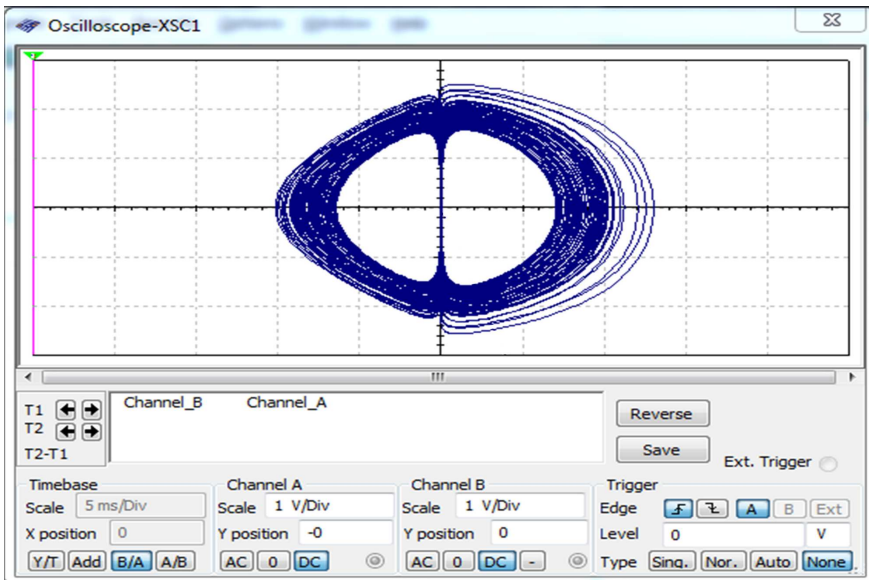
Figure 10: MultiSIM 10 simulation of the system in (y, z)-plane
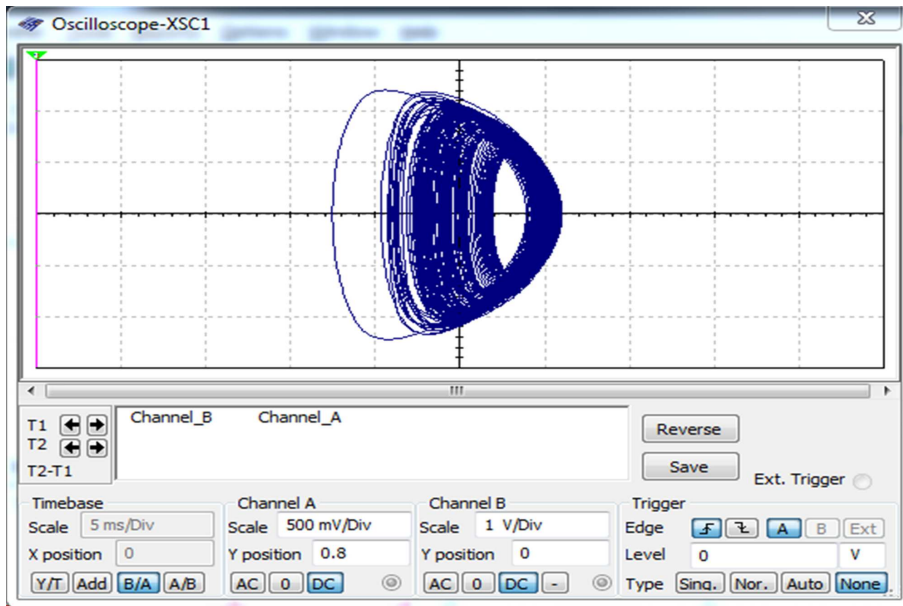
Figure 11: MultiSIM 10 simulation of the system in (x, z)-plane

4. Synchronization results for the new chaotic system with axe-shaped equilibrium

In this section, we design an adaptive synchronizing law for achieving global synchronization of a pair of identical new chaotic systems with axe-shaped equilibrium points (called as the *drive* and *response* systems).

As the drive system, we take the new system with axe-shaped equilibrium given by the dynamics

$$\begin{cases} \dot{x}_1 &= z_1, \\ \dot{y}_1 &= -z_1(-x_1^2 - ay_1 + by_1^2 + cx_1z_1), \\ \dot{z}_1 &= 4|x_1| + 4|y_1| + x_1y_1 - 10. \end{cases} \quad (10)$$

In Eq. (10), $X_1 = (x_1, y_1, z_1)$ represents the state of the drive system and a, b are unknown parameters of the system.

As the response system, we take the new system with axe-shaped equilibrium with controls given by the dynamics

$$\begin{cases} \dot{x}_2 &= z_2 + u_x, \\ \dot{y}_2 &= -z_2(-x_2^2 - ay_2 + by_2^2 + cx_2z_2) + u_y, \\ \dot{z}_2 &= 4|x_2| + 4|y_2| + x_2y_2 - 10 + u_z. \end{cases} \quad (11)$$

In Eq. (11), $X_2 = (x_2, y_2, z_2)$ represents the state of the response system and $u = (u_x, u_y, u_z)$ is the adaptive control to be determined.

We define the synchronization error between the state responses X_1 and X_2 as

$$\begin{cases} e_x &= x_2 - x_1, \\ e_y &= y_2 - y_1, \\ e_z &= z_2 - z_1. \end{cases} \tag{12}$$

It is easy to determine the error dynamics as follows:

$$\begin{cases} \dot{e}_x &= e_z + u_x, \\ \dot{e}_y &= z_2 x_2^2 - z_1 x_1^2 + a(y_2 z_2 - y_1 z_1) - b(y_2^2 z_2 - y_1^2 z_1) \\ &\quad - c(x_2 z_2^2 - x_1 z_1^2) + u_y, \\ \dot{e}_z &= 4(|x_2| - |x_1| + |y_2| - |y_1|) + x_2 y_2 - x_1 y_1 + u_z. \end{cases} \tag{13}$$

As an adaptive control, we consider the feedback law

$$\begin{cases} u_x &= -e_z - k_x e_x, \\ u_y &= -z_2 x_2^2 + z_1 x_1^2 - \alpha(t)(y_2 z_2 - y_1 z_1) + \beta(t)(y_2^2 z_2 - y_1^2 z_1) \\ &\quad + \gamma(t)(x_2 z_2^2 - x_1 z_1^2) - k_y e_y, \\ u_z &= -4(|x_2| - |x_1| + |y_2| - |y_1|) - x_2 y_2 + x_1 y_1 - k_z e_z. \end{cases} \tag{14}$$

In (14), $(\alpha(t), \beta(t), \gamma(t))$ is an estimate of (a, b, c) and $k_x, k_y, k_z \in \mathbf{R}^+$.

When we implement the feedback control law (14), we obtain the closed-loop synchronization error dynamics as

$$\begin{cases} \dot{e}_x &= -k_x e_x, \\ \dot{e}_y &= [a - \alpha(t)](y_2 z_2 - y_1 z_1) - [b - \beta(t)](y_2^2 z_2 - y_1^2 z_1) \\ &\quad - [c - \gamma(t)](x_2 z_2^2 - x_1 z_1^2) - k_y e_y, \\ \dot{e}_z &= -k_z e_z. \end{cases} \tag{15}$$

To simplify the closed-loop dynamics (15), we set

$$\begin{aligned} e_a &= a - \alpha(t), \\ e_b &= b - \beta(t), \\ e_c &= c - \gamma(t). \end{aligned} \tag{16}$$

Then (15) simplifies into the error dynamics

$$
\begin{cases}
\dot{e}_x = -k_x e_x, \\
\dot{e}_y = e_a(y_2 z_2 - y_1 z_1) - e_b(y_2^2 z_2 - y_1^2 z_1) \\
\qquad - e_c(x_2 z_2^2 - x_1 z_1^2) - k_y e_y, \\
\dot{e}_z = -k_z e_z.
\end{cases}
\tag{17}
$$

It is also easy to verify that

$$
\dot{e}_a = -\dot{\alpha}, \qquad \dot{e}_b = -\dot{\beta}, \qquad \dot{e}_c = -\dot{\gamma}.
\tag{18}
$$

We consider the quadratic Lyapunov function candidate

$$
V(e_x, e_y, e_z, e_a, e_b, e_c) = 0.5(e_x^2 + e_y^2 + e_z^2 + e_a^2 + e_b^2 + e_c^2).
\tag{19}
$$

Time-derivative of V along the dynamics (17) and (18) is calculated as follows.

$$
\begin{aligned}
\dot{V} =\ & -k_x e_x^2 - k_y e_y^2 - k_z e_z^2 + e_a[e_y(y_2 z_2 - y_1 z_1) - \dot{\alpha}], \\
& + e_b[-e_y(y_2^2 z_2 - y_1^2 z_1) - \dot{\beta}] + e_c[-e_y(x_2 z_2^2 - x_1 z_1^2) - \dot{\gamma}].
\end{aligned}
\tag{20}
$$

We consider the following dynamics for the parameter updates.

$$
\begin{cases}
\dot{\alpha} = e_y(y_2 z_2 - y_1 z_1), \\
\dot{\beta} = -e_y(y_2^2 z_2 - y_1^2 z_1), \\
\dot{\gamma} = -e_y(x_2 z_2^2 - x_1 z_1^2).
\end{cases}
\tag{21}
$$

Theorem 1 *The new chaotic systems with axe-shaped equilibrium points given by the dynamics (10) and (11) are globally and asymptotically synchronized by the adaptive control law 14) and the parameter update law (21) where $k_x, k_y, k_z \in \mathbf{R}^+$.*

Proof. It is an easy observation that the candidate Lyapunov function V defined via Eq. (19) is positive definite on $\mathbf{R}^6$.

Furthermore, when we substitute (21) into (20), we obtain the time-derivative of V as

$$
\dot{V} = -k_x e_x^2 - k_y e_y^2 - k_z e_z^2.
\tag{22}
$$

Thus, $\dot{V}$ is a negative semi-definite function on $\mathbf{R}^3$.

We set $K = \min\{k_x, k_y, k_z\}$ and $\mathbf{e} = (e_x, e_y, e_z)$.

Then we get $\dot{V} \leqslant -K|\mathbf{e}|^2$, which can be expressed as

$$K|\mathbf{e}(t)|^2 \leqslant -\dot{V}. \tag{23}$$

By integration of the above inequality, we deduce that

$$K \int_0^t |\mathbf{e}(\tau)|^2 \mathrm{d}\tau \leqslant V(0) - V(t). \tag{24}$$

Thus, it follows that $\mathbf{e}(t) \in \mathbf{L}_2$.

Using (17), it can be deduced that $\dot{\mathbf{e}} \in \mathbf{L}_\infty$.

As a consequence of Barbalat's lemma [50], $\mathbf{e}(t) \to 0$ as $t \to \infty$ for all values of $\mathbf{e}(0) \in \mathbf{R}^3$.   □

For numerical simulations, we take the gain constants as $(k_1, k_2, k_3) = (10, 10, 10)$ and the system parameter values as $(a, b, c) = (6, 0.2, 0.1)$.

As initial states of the systems (10) and (11), we take $(x_1(0), y_1(0), z_1(0)) = (1.5, 0.6, 0.1)$ and $(x_2(0), y_2(0), z_2(0)) = (0.4, 0.3, 2.4)$.

Also, we take $(\alpha(0), \beta(0), \gamma(0)) = (1.2, 0.5, 3.1)$.

Figures 12–14 show the complete synchronization of (10) and (11), while Figure 15 shows the time-history of the synchronization error $\mathbf{e}$.

Figure 12: MATLAB simulation showing synchronization of the states x_1 and x_2 of the systems (10) and (11)

Figure 13: MATLAB simulation showing synchronization of the states y_1 and y_2 of the systems (10) and (11)
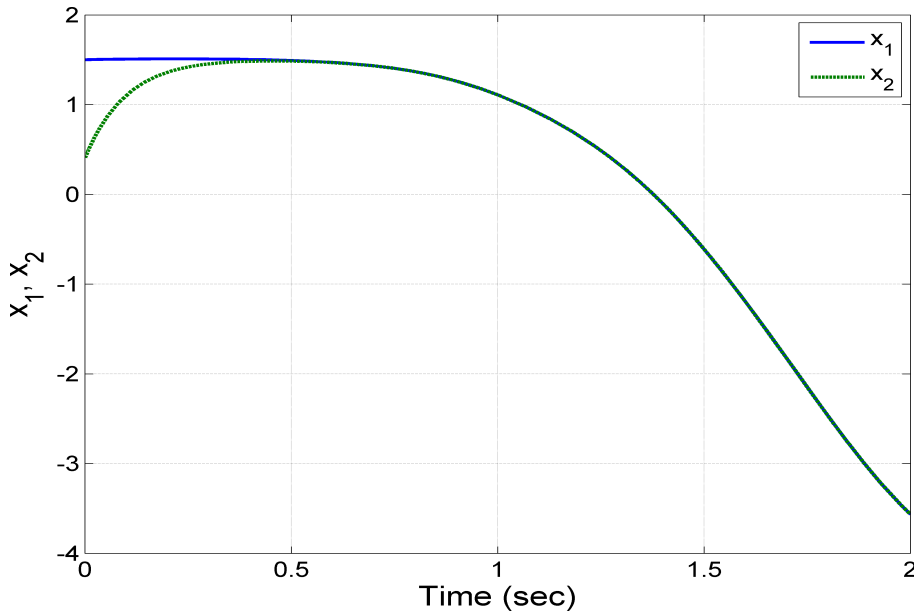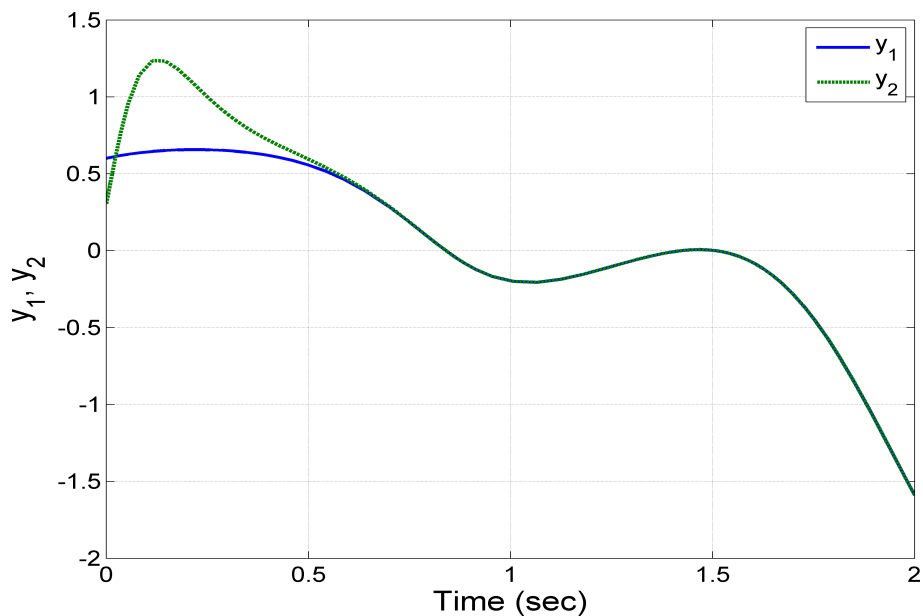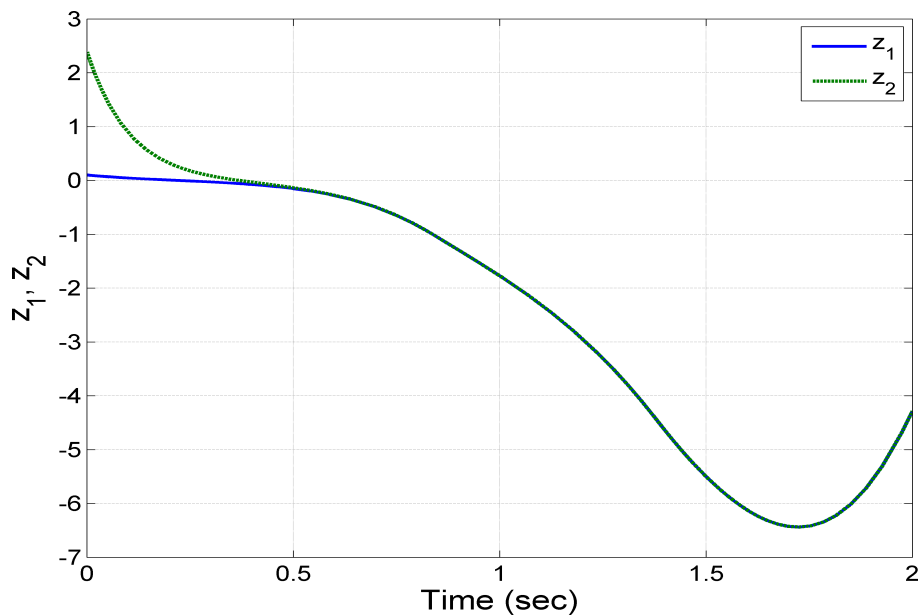

Figure 14: MATLAB simulation showing synchronization of the states x_1 and x_2 of the systems (10) and (11)
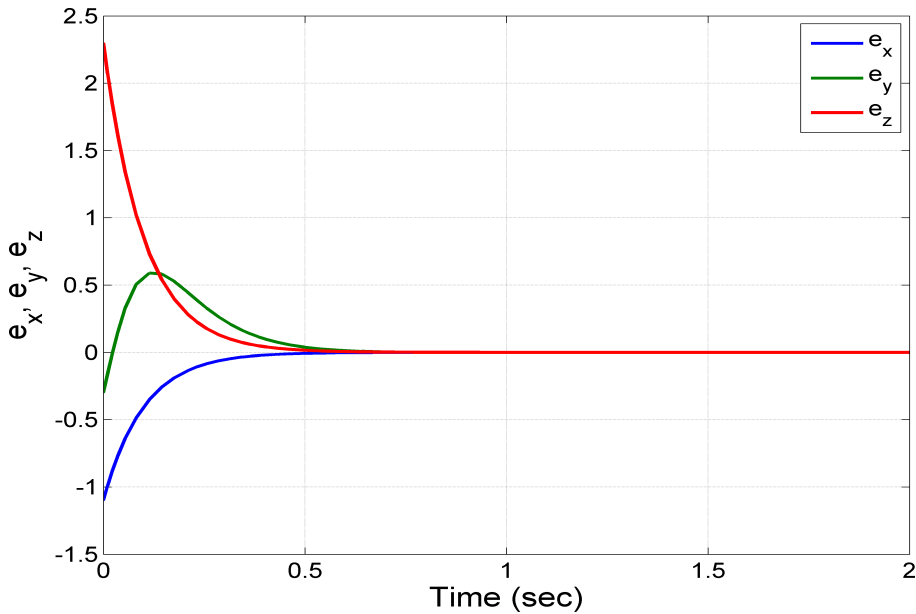
Figure 15: MATLAB simulation showing the time-history of the synchronization error **e** between the systems (10) and (11)

5. Conclusions

In this research work, we reported a chaotic system with an axe-shaped curve of equilibrium points. In addition to detailing the dynamic properties of the new system, an electronic circuit implementation of the new chaotic system with axe-shaped equilibrium was also reported to check its feasibility. As a control application, we gave results for the synchronization of the new system possessing an axe-shaped curve of equilibrium points.

References

[1] H. Liu, B. Ren, Q. Zhao and N. Li: Characterizing the optical chaos in a special type of small networks of semiconductor lasers using permutation entropy, *Optics Communications,* **359** (2016), 79–84.

[2] T. Wu, W. Sun, X. Zhang and S. Zhang: Concealment of time delay signature of chaotic output in a slave semicondutor laser with chaos laser injection, *Optics Communications,* **381** (2016), 174–179.

[3] J. ZHANG and X. LIAO: Synchronization and chaos in coupled memristor-based FitzHugh-Naguom circuits with memristor synapse, *AEU-International Journal of Electronics and Communications,* **75** (2017), 82–90.

[4] W. HU, D. DING, Y. ZHANG, N. WANG and D. LIANG: Hopf bifurcation and chaos in a fractional order delayed memristor-based chaotic circuit system, *Optik,* **130** (2017), 189–200.

[5] S. VAIDYANATHAN: Adaptive synchronization of novel 3-D chemical chaotic reactor systems, *International Journal of ChemTech Research,* **8**(7), (2015), 159–171.

[6] D. GU, Z. LIU, J. LI, Z. XIE, C. TAO and Y. WANG: Intensification of chaotic mixing in a stirred tank with a punched rigid-flexible impeller and a chaotic motor, *Chemical Engineering and Processing: Process Intensification,* **122** (2017), 1–9.

[7] O.I. TACHA, C.K. VOLOS, I.M. KYPRIANIDIS, I.N. STOUBOULOS, S. VAIDYANATHAN and V.T. PHAM: Analysis, adaptive control and circuit simulation of a novel nonlinear finance system, *Applied Mathematics and Computation, 276* (2016), 200–217.

[8] S. VAIDYANATHAN: Hyperchaos, qualitative analysis, control and synchronisation of a ten-term 4-D hyperchaotic system with an exponential nonlinearity and three quadratic nonlinearities, *International Journal of Modelling, Identification and Control,* **23**(4), (2015), 380–392.

[9] S. VAIDYANATHAN: Adaptive controller and synchronizer design for the Qi-Chen chaotic system, *Lecture Notes of the Institute for Computer Sciences, Social-Informatics and Telecommunications Engineering,* **85** (2012), 124–133.

[10] S. VAIDYANATHAN: Analysis, control, and synchronization of a 3-D novel jerk chaotic system with two quadratic nonlinearities, *Kyungpook Mathematical Journal,* **55**(3), (2015), 563–586.

[11] S. PAKIRISWAMY and S. VAIDYANATHAN: Generalized projective synchronization of three-scroll chaotic systems via active control, *Lecture Notes of the Institute for Computer Sciences, Social-Informatics and Telecommunications Engineering,* **85** (2012), 146–155.

[12] S. VAIDYANATHAN: Analysis and synchronization of the hyperchaotic Yujun systems via sliding mode control, *Advances in Intelligent Systems and Computing,* **176** (2012), 329–337.

[13] S. VAIDYANATHAN and S. RASAPPAN: Hybrid synchronization of hyperchaotic Qi and Lü systems by nonlinear control, *Communications in Computer and Information Science,* **131** (2011), 585–593.

[14] S. VAIDYANATHAN: Output regulation of the forced Van der Pol chaotic oscillator via adaptive control method, *International Journal of PharmTech Research,* **8**(6), (2015), 106–116.

[15] S. VAIDYANATHAN: Global chaos synchronization of the forced Van der Pol chaotic oscillators via adaptive control method, *International Journal of PharmTech Research,* **8**(6), (2015), 156–166.

[16] S. VAIDYANATHAN: Synchronization of 3-cells cellular neural network (CNN) attractors via adaptive control method, *International Journal of PharmTech Research,* **8**(5), (2015), 946–955.

[17] S. VAIDYANATHAN: Lotka-Volterra population biology models with negative feedback and their ecological monitoring, *International Journal of PharmTech Research,* **8**(5), (2015), 974–981.

[18] S. VAIDYANATHAN: Chaos in neurons and synchronization of Birkhoff-Shaw strange chaotic attractors via adaptive control, *International Journal of PharmTech Research,* **8**(6), (2015), 1–11.

[19] S. VAIDYANATHAN: Adaptive control of the FitzHugh-Nagumo chaotic neuron model, *International Journal of PharmTech Research,* **8**(6), (2015), 117–127.

[20] S. VAIDYANATHAN, C.K. VOLOS, K. RAJAGOPAL, I.M. KYPRIANIDIS and I.N. STOUBOULOS: Adaptive backstepping controller design for the anti-synchronization of identical WINDMI chaotic systems with unknown parameters and its SPICE implementation, *Journal of Engineering Science and Technology Review,* **8**(2), (2015), 74–82.

[21] S. VAIDYANATHAN, A.T. AZAR, K. RAJAGOPAL, A. SAMBAS, S. KACAR and U. CAVUSOGLU: A new hyperchaotic temperature fluctuations model, its circuit simulation, FPGA implementation and an application to image encryption, *International Journal of Simulation and Process Modelling,* **13** (3), (2018), 281–296.

[22] S. VAIDYANATHAN, A. AKGUL, S. KACAR and U. CAVUSOGLU: A new 4-D chaotic hyperjerk system, its synchronization, circuit design and applications in RNG, image encryption and chaos-based steganography, *European Physical Journal Plus,* **133**(2), (2018), Article ID 46.

[23] P. DALTZIS, S. VAIDYANATHAN, V.T. PHAM, C. VOLOS, E. NISTAZA-KIS and G. TOMBRAS: Hyperchaotic attractor in a novel hyperjerk system with two nonlinearities, *Circuits, Systems and Signal Processing,* **37** (2018), 613–635.

[24] V.T. PHAM, S. JAFARI, C. VOLOS, A. GIAKOUMIS, S. VAIDYANATHAN and T. KAPITANIAK: A chaotic system with equilibria located on the rounded square loop and its circuit implementation, *IEEE Transactions on Circuits and Systems-II: Express Briefs,* **63** (9), (2016), 878–882.

[25] C. VOLOS, J.O. MAAITA, S. VAIDYANATHAN, V.T. PHAM, I. STOU-BOULOS and I. KYPRIANIDIS: A novel four-dimensional hyperchaotic four-wing system with a saddle-focus equilibrium, *IEEE Transactions on Circuits and Systems-II: Express Briefs,* **64** (3), (2017), 339–343.

[26] S. VAIDYANATHAN, S. JAFARI, V.T. PHAM, A.T. AZAR and F.E. AL-SAADI: A 4-D chaotic hyperjerk system with a hidden attractor, adaptive backstepping control and circuit design, *Archives of Control Sciences,* **28** (2), (2018), 239–254.

[27] A. SAMBAS, S. VAIDYANATHAN, M. MAMAT, W.S. SANJAYA and R.P. PRASTIO: Design, analysis of the Genesio-Tesi chaotic system and its electronic experimental implementation, *International Journal of Control Theory and Applications,* **9** (1), (2016), 141–149.

[28] S. VAIDYANATHAN, A. SAMBAS, M. MAMAT and M. SANJAYA WS: Analysis, synchronisation and circuit implementation of a novel jerk chaotic system and its application for voice encryption. *International Journal of Modelling, Identification and Control,* **28** (2), (2017), 153–166.

[29] X. ZHANG and X. WANG: Multiple-image encryption algorithm based on mixed image element and chaos, *Computers & Electrical Engineering,* **62** (2017), 401–413.

[30] U. CAVUSOGLU, A. AKGUL, A. ZENGIN and I. PEHLIVAN: The design and implementation of hybrid RSA algorithm using a novel chaos based RNG, *Chaos, Solitons & Fractals,* **104** (2017), 655–667.

[31] S. VAIDYANATHAN, A. SAMBAS, M. MAMAT and M. SANJAYA WS: A new three-dimensional chaotic system with a hidden attractor, circuit design and application in wireless mobile robot, *Archives of Control Sciences,* **27** (4), (2017), 541–554.

[32] Z. SUN, L. SI, Z. SHANG and J. LEI: Finite-time synchronization of chaotic PMSM systems for secure communication and parameter identification, *Optik,* **157** (2018), 43–55.

[33] H. JIA, Z. GUO, G. QI and Z. CHEN: Analysis of a four-wing fractional-order chaotic system via frequency-domain and time-domain approaches and circuit implementation for secure communication, *Optik,* **155** (2018), 233–241.

[34] C. LI, J.C. SPROTT and W. THIOC: Bistability in a hyperchaotic system with a line equilibrium, *Journal of Experimental and Theoretical Physics,* **118**(3), (2014), 494–500.

[35] S.T. KINGNI, V.T. PHAM, S. JAFARI and P. WOAFO: A chaotic system with an infinite number of equilibrium points located on a line and on a hyperbola and its fractional-order form, *Chaos, Solitons & Fractals,* **99** (2017), 209–218.

[36] S. VAIDYANATHAN: A novel 5-D hyperchaotic system with a line of equilibrium points and its adaptive control, *Studies in Computational Intelligence,* **636** (2016), 471–494.

[37] T. GOTTHANS and J. PETRZELA: New class of chaotic systems with circular equilibrium, *Nonlinear Dynamics,* **81**(3), (2015), 1143–1149.

[38] V.T. PHAM, S. VAIDYANATHAN, C.K. VOLOS, S. JAFARI and T. GOTTHANS: A three-dimensional chaotic system with square equilibrium and noequilibrium, *Studies in Computational Intelligence,* **688** (2017), 613–635.

[39] V.T. PHAM, S. JAFARI, C. VOLOS, A. GIAKOUMIS, S. VAIDYANATHAN and T. KAPITANIAK: A chaotic system with equilibria located on the rounded square loop and its circuit implementation, *IEEE Transactions on Circuits and Systems II: Express Briefs,* **63**(9), (2016), 878–882.

[40] V.T. PHAM, S. JAFARI, X. WANG and J. MA: A chaotic system with different shapes of equilibria, *International Journal of Bifurcation and Chaos,* **26** (2016), Article ID 1650069.

[41] X. WANG, V.T. PHAM and C. VOLOS: Dynamics, circuit design and synchronization of a new chaotic system with closed curve equilibrium, *Complexity,* 2017 (2017), Article ID 7138971.

[42] G.A. LEONOV, N.V. KUZNETSOV and V.I. VAGAITSEV: Localication of hidden Chua's attractors, *Physics Letters A,* **375**(23), (2011), 2230–2233.

[43] M.F. DANCA, F. KUZNETSOV and G. CHEN: Unusual dynamics and hidden attractors of the Rabinovich-Fabricant system, *Nonlinear Dynamics,* **88**(1), (2017), 791–805.

[44] V.T. PHAM, S. VAIDYANATHAN, C.K. VOLOS, T.M. HOANG and V.V. YEM: Dynamics, synchronization and SPICE implementation of a memristive system with hidden hyperchaotic attractor, *Studies in Fuzziness and Soft Computing,* **337** (2017), 3–34.

[45] S. VAIDYANATHAN: Adaptive control and synchronization of a rod-type plasma torch chaotic system via backstepping control method. *Studies in Computational Intelligence,* **636** (2016), 553–578.

[46] S. VAIDYANATHAN: Analysis, adaptive control and synchronization of a novel 3-D chaotic system with a quartic nonlinearity. *Studies in Computational Intelligence,* **636** (2016), 579–600.

[47] S. VAIDYANATHAN, A.T. AZAR and A. BOULKROUNE: A novel 4-D hyperchaotic system with two quadratic nonlinearities and its adaptive synchronisation, *International Journal of Automation and Control,* **12**(1), (2018), 5–26.

[48] N. KUZNETSOV: The Lyapunov dimension and its estimation via the Leonov method, *Physics Letters A*, **380** (2016), 2142–2149.

[49] A. WOLF, J.B. SWIFT, H.L. SWINNEY and J. VASTANO: Determining Lyapunov exponents from a time series, *Physica D*, **16** (1985), 285–317.

[50] H.K. KHALIL: Nonlinear Systems. New York, Prentice Hall, 2002.